MPMI Vol. 37, No. 3, 2024, pp. 250–263, https://doi.org/10.1094/MPMI-09-23-0139-FI

Novel Secreted Effectors Conserved Among Smut Fungi Contribute to the Virulence of *Ustilago maydis*

Mariana Schuster,[1,2,†] Gabriel Schweizer,[1,3] Stefanie Reißmann,[1] Petra Happel,[1] Daniela Aßmann,[1] Nicole Rössel,[1] Ulrich Güldener,[4] Gertrud Mannhaupt,[1] Nicole Ludwig,[1,5] Sarah Winterberg,[1] Clément Pellegrin,[1] Shigeyuki Tanaka,[1] Volker Vincon,[1] Libera Lo Presti,[1] Lei Wang,[1] Lena Bender,[1,6] Carla Gonzalez,[1] Miroslav Vranes,[7] Jörg Kämper,[7] Kyungyong Seong,[8] Ksenia Krasileva,[8] and Regine Kahmann[1]

[1] Max Planck Institute for Terrestrial Microbiology, 35043 Marburg, Germany
[2] Leibniz Institute of Plant Biochemistry, Weinberg 3, 06120 Halle, Germany
[3] Independent Data Lab UG, 80937 Munich, Germany
[4] Deutsches Herzzentrum München, Technische Universität München, 80636 München, Germany
[5] Research & Development, Weed Control Bayer AG, Crop Science Division, 65926 Frankfurt am Main, Germany
[6] Department of Pharmaceutics and Biopharmaceutics, Phillips-University Marburg, 35037 Marburg, Germany
[7] Karlsruhe Institute of Technology, Institute for Applied Biosciences, Department of Genetics, 76131 Karlsruhe, Germany
[8] Department of Plant and Microbial Biology, University of California, Berkeley, CA 94720, U.S.A.

Accepted for publication 26 February 2024.

Fungal pathogens deploy a set of molecules (proteins, specialized metabolites, and sRNAs), so-called effectors, to aid the infection process. In comparison to other plant pathogens, smut fungi have small genomes and secretomes of 20 Mb and around 500 proteins, respectively. Previous comparative genomic studies have shown that many secreted effector proteins without known domains, i.e., novel, are conserved only in the Ustilaginaceae family. By analyzing the secretomes of 11 species within Ustilaginaceae, we identified 53 core homologous groups commonly present in this lineage. By collecting existing mutants and generating additional ones, we gathered 44 *Ustilago maydis* strains lacking single core effectors as well as 9 strains containing multiple deletions of core effector gene families. Pathogenicity assays revealed that 20 of these 53 mutant strains were affected in virulence. Among the 33 mutants that had no obvious phenotypic changes, 13 carried additional, sequence-divergent, structurally similar paralogs. We report a virulence contribution of seven previously uncharacterized single core effectors and of one effector family. Our results help to prioritize effectors for understanding *U. maydis* virulence and provide genetic resources for further characterization.

Keywords: biotrophy, comparative genomics, CRISPR-Cas9, novel core effectors, smut fungi, *Ustilago maydis*, virulence

Biotrophic fungal plant pathogens cause significant losses in agriculture (Fisher et al. 2020; Savary et al. 2019). They rely on living plant tissue for colonization and establish intimate interactions with their hosts. Understanding the molecular mechanisms by which these pathogens cause disease is considered an important first step toward disease management (Depotter and Doehlemann 2020).

Smut fungi are a group of important biotrophic plant pathogens with relatively small genomes of about 20 Mb (Benevenuto et al. 2018; Zuo et al. 2019). The term "smut" refers to the dark and powdery appearance of the fungal spores released from infected plants and does not constitute a taxonomic term (Begerow et al. 2014). Most "true smut lineages" are grass pathogens and belong to Tilletiales and the Ustilaginaceae family (Begerow et al. 2014; Vánky 2013). Among members of the Ustilaginaceae family, there are important crop plant pathogens, and several of these have been used as model systems to study the interaction of biotrophic fungi with host plants. Such examples include *Ustilago maydis*, *Ustilago hordei*, and *Sporisorium reilianum* f. sp. *zeae* causing corn smut, covered smut in barley, and maize head smut, respectively (Ökmen et al. 2021; Xia et al. 2020; Zuo et al. 2019). Other members like *Sporisorium reilianum* f. sp. *reilianum* infecting sorghum, *Ustilago tritici* causing loose smut of wheat, *Ustilago esculenta* infecting Manchurian rice grass (*Zizania latifolia*), *Ustilago bromivora* infecting *Brachypodium distachion*, and *Sporisorium scitamineum*

†Corresponding author: M. Schuster; mariana.schuster@ipb-halle.de

M. Schuster and G. Schweizer contributed equally.

Current address for S. Winterberg: Phillips-University Marburg, Institute of Anatomy and Cell Biology, Robert-Koch-Strasse 8, 35037 Marburg, Germany.

Current address for C. Pellegrin: European Commission, Joint Research Centre (JRC), B-2440 Geel, Belgium.

Current address for S. Tanaka: Faculty of Agriculture, Setsunan University, Laboratory of Plant Environmental Microbiology, 45-1 Nagaotoge-cho, Hirakata City, Osaka 573-0101, Japan.

Current address for L. Lo Presti: Eberhard-Karls-Universität Tübingen, Exzellenzcluster CMFI, Auf der Morgenstelle 28E, 72076 Tübingen, Germany.

Funding: We acknowledge generous support by the Max Planck Society.

***e*-Xtra:** Supplementary material is available online.

The author(s) declare no conflict of interest.

causing sugarcane smut (Agrios 2005) have been mostly used for comparative analyses (Benevenuto et al. 2018; Dutheil et al. 2016; Laurie et al. 2012; Lefebvre et al. 2013; Schuster et al. 2018; Schweizer et al. 2018; Sharma et al. 2014, 2015; Ye et al. 2017). *Melanopsichium pennsylvanicum* is an exception among the Ustilaginaceae in its ability to infect dicot *Persicaria* species (Begerow et al. 2000, 2006, 2014).

In recent years, secreted effectors have surfaced as virulence determinants in biotrophic pathogens (Jaswal et al. 2020; Lo Presti et al. 2015; Lorrain et al. 2019; Ökmen and Doehlemann 2014; Wang et al. 2017). The study of effectors and how they modulate plant processes has become an important line of research. Effectors are commonly defined as molecules secreted by the pathogen that aid in infection by suppressing plant defense responses, protecting the pathogen from defense compounds, modulating host physiology to the benefit of the pathogen, and contributing to host specificity, among other roles (Borah et al. 2018; Liu et al. 2019; Rovenich et al. 2014; Uhse and Djamei 2018). Many studied effectors are proteins that lack known domains, their expression is restricted to colonization, and their individual contribution to virulence is typically small (Lo Presti et al. 2015; Lorrain et al. 2019; Win et al. 2012). Effectors can function outside the cell and/or be taken up by plant cells and modulate plant processes in the cytoplasm or subcellular compartments (Khan et al. 2018; Lo Presti and Kahmann 2017; Petre and Kamoun 2014; Wang et al. 2017). So far, most functional analyses of secreted effector proteins of true smut fungi have been performed in *U. maydis*, because this pathosystem offers a highly developed toolbox for genome manipulation and allows virulence assays to be conducted in seedlings in about 2 weeks (Lanver et al. 2017; Olicón-Hernández et al. 2019). An assessment of virulence in *U. maydis* is additionally facilitated by the availability of a solopathogenic haploid strain (SG200) that causes disease without a mating partner (Kämper et al. 2006).

With the availability of the *U. maydis* genome sequence, the secretome of 476 proteins was predicted, and their expression was shown to be linked to discrete stages of colonization (Lanver et al. 2018; Schuster et al. 2018). Of these putative effector proteins, about 50% lack known domains, and we designate them as novel (Schuster et al. 2018). So far, only five secreted *U. maydis* effector proteins with known domains have been molecularly characterized in detail: a chorismate mutase, a fungalysin metalloprotease, a 1,3-β-glucanase, a ribonuclease, and a PR-1 like protein (Djamei et al. 2011; Han et al. 2019; Lin et al. 2023; Ökmen et al. 2018, 2022, 2023). About 20% of the novel effectors reside in clusters in the genome. Deletion of such effector gene clusters has helped uncover the link between novel effectors and virulence (Kämper et al. 2006; Navarrete et al. 2021; Schirawski et al. 2010), and molecular studies on one of the clusters revealed functional redundancy among its members (Bindics et al. 2022). To date, virulence assays of single-deletion mutants have helped uncover the differential contribution of more than 30 novel effectors to virulence (Schilling et al. 2014; Seitner et al. 2018; Stirnberg and Djamei 2016; Uhse et al. 2018), and the molecular functions of many of them have been elucidated (Darino et al. 2021; Fukada et al. 2021; Hemetsberger et al. 2012; Hoang et al. 2021; Huang et al. 2024; Khan et al. 2023; Ludwig et al. 2021; Ma et al. 2018; Mueller et al. 2013; Navarrete et al. 2022; Redkar et al. 2015b; Tanaka et al. 2014, 2020; Weiland et al. 2023; Zuo et al. 2023). Most of these effectors have been described as targeting discrete host pathways, and findings highlight the TOPLESS class of co-repressors as a hub for *U. maydis* effector action (Khan et al. 2023). Remarkably, five of the novel effectors were shown to form a protein complex together with two fungal transmembrane proteins. This protein complex has an essential virulence-promoting function likely associated with effector delivery (Ludwig et al. 2021).

Except for Jsi1, all characterized *U. maydis* effectors are present in several smut fungi (Darino et al. 2021; Fukada et al. 2021; Schuster et al. 2018; Tanaka et al. 2020; Weiland et al. 2023). Such effectors with homologs present across species have been speculated to hold important and conserved virulence functions in different host plants (Depotter and Doehlemann 2020).

Recent advances in structure prediction allowed effectors to be grouped within and across fungal pathogens based on shared fold similarity (Outram et al. 2022; Seong and Krasileva 2023; Yan et al. 2023; Yu et al. 2024). In *U. maydis*, 69 effector fold groups have been identified, with seemingly unrelated secreted proteins clustering in genomic segments while having divergent expression patterns and rapid evolution of protein surfaces (Seong and Krasileva 2023). Moreover, nearly half of the *U. maydis* secreted proteins exist as structural singletons lacking stable folds, robust structure models, or detectable structural similarity to other proteins (Seong and Krasileva 2023). This suggests that while gene duplication and structural conservation enable pathogens such as *U. maydis* to expand their effector repertoires, functional studies remain critical for understanding the relative contribution of effectors to virulence.

In this study, we have determined the virulence contribution of all novel conserved effectors in *U. maydis* to identify new effector candidates for molecular characterization. To this end, we performed a comparative genomics analysis with secreted proteins of 11 plant pathogenic Ustilaginaceae species and defined 53 homologous groups of effectors conserved in all studied species, which we term core. *U. maydis* has a single gene in 44 of these 53 groups and 2 to 9 paralogs in 9 groups that form gene families. For the effectors already published, we acquired the corresponding knockout mutants. For the uncharacterized ones, we generated 31 single null mutants as well as 8 multigene null mutants. In total, 44 *U. maydis* strains lacking single effector candidates and 9 multigene knockout strains were tested in parallel for virulence. We show that 20 core effector groups contribute to virulence in the *U. maydis*–maize system.

Results

Fifty-three groups of novel effectors are core effectors in smut fungi

To uncover conserved effector proteins in smut fungi, we used the available proteomes of *U. bromivora*, *U. hordei*, *U. maydis*, *S. scitamineum*, *S. reilianum* f. sp. *reilianum*, and *S. reilianum* f. sp. *zeae* (Supplementary Table S1). To obtain high-quality data from the dicot-infecting smut, we resequenced the genome of *M. pennsylvanicum*, which we then included in the analysis (Supplementary Table S1) First, we identified putative secreted proteins by predicting the presence of the secretion signal peptide and the absence of transmembrane domains and endoplasmic reticulum (ER) retention motif. This led to the identification of 379 secreted proteins in *M. pennsylvanicum*, 414 in *U. bromivora*, 396 in *U. hordei*, 471 in *U. maydis*, 469 in *S. scitamineum*, 482 in *S. reilianum* f. sp. *reilianum*, and 470 in *S. reilianum* f. sp. *zeae* (Fig. 1A; Supplementary Table S1). We then curated 462 homologous groups by clustering the secreted proteins with OrthoMCL (Enright et al. 2002; Supplementary Table S2). Based on InterPro (Finn et al. 2017) domain predictions, each homologous group was classified into two categories: either with predicted functional domains or without predicted functional domains (novel). Of the 462 homologous groups, 214 belonged to the category with functional domains and 248 were novel (Supplementary Table S2). Of all groups, 139 contained proteins from all 7 species and were therefore considered core groups (Fig. 1A; Supplementary Table S2). Of these 139 core groups, 86 groups contained effectors with known domains, while the other 53 groups contained only novel proteins

(Fig. 1A; Supplementary Table S2). *U. maydis* had a single gene in 44 of these 53 novel core groups; for the remining 9 groups, *U. maydis* had 2 to 9 paralogs forming gene families (Supplementary Table S3). The largest of these families contains 9 of the 11 members of the previously described effector family 1 (Eff1) (Khrunyk et al. 2010). Following this notation, we termed the newly defined effector families Eff2 to Eff9 (Table 1). Finally, the genomes of *Ustilago trichophora* (Zambanini et al. 2016), *U. esculenta* (Ye et al. 2017), *U. tritici*, and an *U. hordei* strain infecting oats (Benevenuto et al. 2018) were used to validate and confirm the existence of 53 core groups (see "Materials and Methods" for details) (Fig. 1B; Supplementary Table S3).

Table 1. Novel core effector families of *Ustilago maydis*

Family name	Genes in the family
Eff1[a]	*UMAG_01796*, *UMAG_11377*, *UMAG_02137*, *UMAG_02138*, *UMAG_02139*, *UMAG_02140*, *UMAG_03313*, *UMAG_03314*, *UMAG_02141*
Eff2	*UMAG_11415*, *UMAG_02535*, *UMAG_11416*, *UMAG_02537*, *UMAG_02538*
Eff3	*UMAG_02229*, *UMAG_10076*
Eff4	*UMAG_03752*, *UMAG_03753*
Eff5	*UMAG_01297*, *UMAG_01298*
Eff6	*UMAG_00961*, *UMAG_02921*
Eff7	*UMAG_00792*, *UMAG_00793*
Eff8	*UMAG_05926*, *UMAG_05928*
Eff9	*UMAG_06440*, *UMAG_12316*

[a] The strain corresponds to the "nine-gene-deletion" mutant, where 9 out of 11 Eff1 family members were deleted.

Obtaining *U. maydis* mutants lacking novel core effectors

In previous studies, 14 of the 44 single novel core effectors and 2 of the 9 gene families had been functionally analyzed by respective gene deletions. These analyses had revealed that 13 of the 16 mutants showed reduced virulence compared with the progenitor strain (Supplementary Table S4).

Based on these existing virulence data on core effector groups, we hypothesized that the remaining groups of novel core *U. maydis* effectors defined in the scope of our study might also have a strong contribution to virulence. We acquired the 16 existing SG200 deletion strains from the respective research groups and verified the gene deletions with Southern blot analyses. We then created single-deletion mutants of the remaining 30 single core effectors either by gene replacement (Kämper 2004) or CRISPR-Cas9 genome editing (Schuster et al. 2016) in the SG200 background. For each of the remaining seven gene families, multigene mutants lacking all family members were generated by CRISPR-Cas9 genome editing. All newly generated mutants were verified either by Southern blot analysis or by sequencing the mutated site.

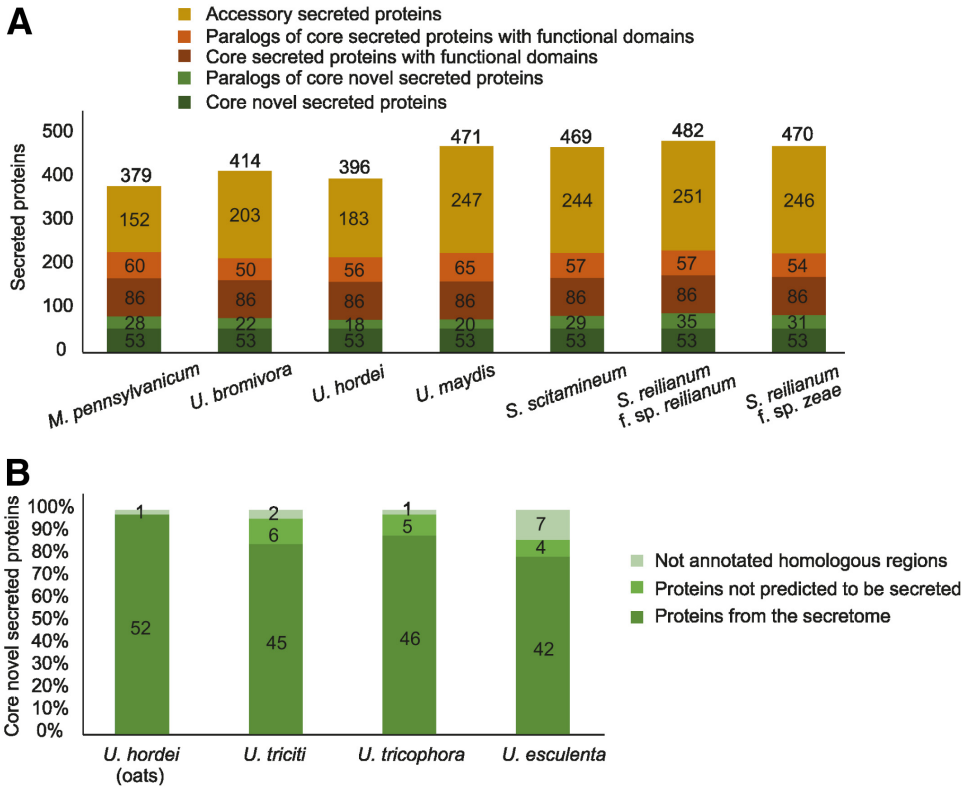

Fig. 1. Composition and conservation of secreted proteins among plant pathogenic smut fungi. **A,** Groups of homologous proteins were built among the secretomes of seven smut fungi using OrthoMCL. The homologous groups were categorized in groups with proteins harboring functional domains and groups containing novel proteins. Among those groups containing proteins from all compared species (core groups), 53 belong to the category novel (dark green) and 86 to the category functional domain (dark orange). Expansions of these groups in each species are depicted with light green for the novel proteins and light orange for the proteins harboring functional domains. Groups where proteins from at least one species were missing are denominated accessory (yellow). **B,** BLAST searches were performed for the core novel effectors in the genomes of four sequenced plant pathogenic smut fungi. Homologous regions from all 53 core novel effectors were found. In most cases, the homologs correspond to secreted proteins (dark green). In some cases, homologs were present but did not belong to the secretome (bright green). In most of these cases, careful analysis of the alignment of the corresponding group led us to propose annotation errors (Supplementary Table S13; Supplementary Fig. S2). In some other cases, homologous regions were found that lacked gene annotation. In these cases, we propose missing annotation (Supplementary Table S13; Supplementary Fig. S2).

Establishing the phenotypes of *U. maydis* mutants lacking novel core effectors

As virulence of previously published core effectors was determined in different laboratories, published virulence phenotypes could not be directly compared. Variability in virulence might be caused by differences in the susceptibility of the host plant varieties used and other variable experimental settings like glasshouse settings. Therefore, we decided to determine the virulence of the 53 core effector mutants in parallel under consistent experimental conditions. Virulence was assessed via syringe injection into 7-day-old maize seedlings of the variety 'Early Golden Bantam' followed by scoring disease symptoms at 12 days postinfection (dpi) (Fig. 2). Virulence was compared with that of the parental strain SG200. Of the 44 single-gene mutants lacking novel core effectors, 19 showed reduced or abolished virulence (Fig. 2; Supplementary Table S4). The complete loss of virulence was seen for mutants lacking *stp1*, *stp2*, *stp3* (Ludwig et al. 2021), *pep1* (Doehlemann et al. 2009), and *cce1/stp4* (Ludwig et al. 2021; Seitner et al. 2018; Fig. 2). The *pit2* mutant previously reported to only induce ligula swelling and small tumors (Mueller et al. 2013) also displayed complete loss of virulence in our assay (Fig. 2). A general reduction of disease in all scored categories was observed after infection with mutants lacking *see1* (Redkar et al. 2015b), *rsp3* (Ma et al. 2018), and *apb73* (Stirnberg and Djamei 2016; Fig. 2). A reduction of strong disease symptoms and an increase in plants without any symptoms was observed for the mutant lacking *sta1* (Tanaka et al. 2020; Fig. 2), while the mutant lacking *UMAG_11062* only showed a reduction of the most severe disease categories (Fig. 2). This analysis newly identified the contribution of novel core effectors to virulence, namely, *UMAG_00054*, *UMAG_00104*, *UMAG_05780*, *UMAG_05932*, *UMAG_11062*, *UMAG_11362*, and *UMAG_11205*.

Of the nine gene family mutants, two displayed reduced virulence (Fig. 2; Supplementary Table S4). This includes the previously characterized *eff1* mutant lacking 9 of the 11 *eff1* family genes (Khrunyk et al. 2010) and the newly identified mutant *eff9*. The *eff9* mutant lacks both *UMAG_06440* and *UMAG_12316* and showed small but significant reduction in all virulence symptoms compared with SG200 (Fig. 2). The remaining seven mutants lacking novel core effector gene families were comparable in virulence to SG200 (Fig. 2).

The significant reduction in virulence of the 21 mutants could have resulted from defects in vegetative growth and development. To evaluate this possibility, we assessed growth and filamentation of all 53 strains in comparison to SG200 (see "Materials and Methods"). A noticeable reduction in colony size in comparison to SG200, indicative of a vegetative growth defect, was not observed for any of the 21 mutant strains with reduced virulence (Supplementary Fig. S1A and B). Reduced filamentous growth, indicative of a developmental defect, was observed in single mutants lacking *see1* (Redkar et al. 2015b),

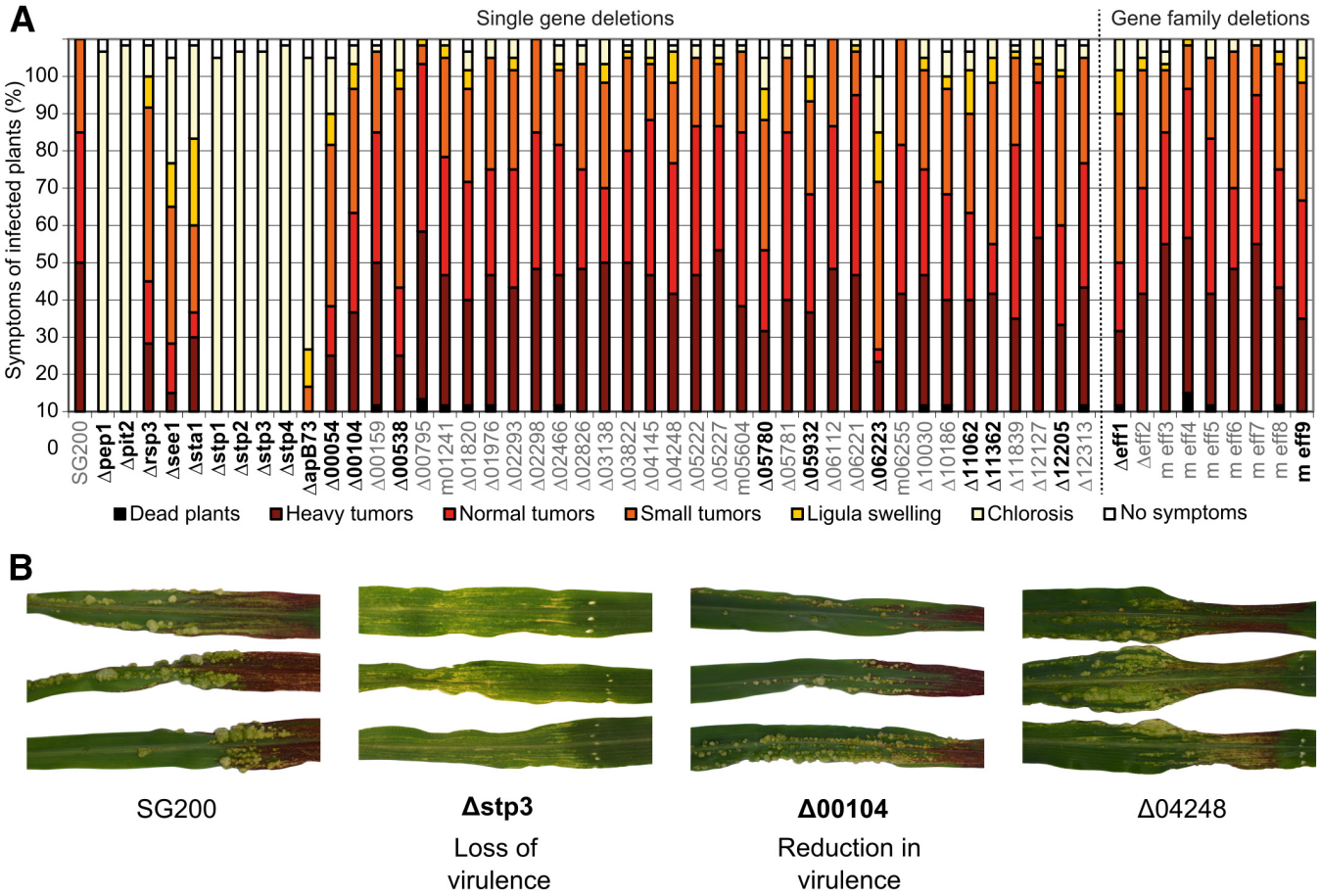

Fig. 2. Virulence phenotype of core novel effectors mutants in *Ustilago maydis*. **A,** Mutants of the 44 single novel core effectors and 9 novel core effector families were generated in SG200. Δ indicates gene replacement, whereas "m" indicates inactivation using CRISPR-Cas9. Sixty 7-day-old maize seedlings per strain were infected, and disease symptoms were scored at 12 days postinfection (dpi). Disease symptoms scores are given below the bar graph and were quantified based on three biological replicates. The mean percentage of plants placed in a certain disease category is indicated. Strain names in black indicate significant differences of disease symptoms between the respective strain and SG200 determined by a Kruskal-Wallis test followed by a Conover-Iman and an adjusted *P* value (Benjamini-Hochberg) < 0.01. Among the deletion mutants, 20 strains presented a statistically significant reduction in disease symptoms in planta, and 5 were not virulent. Statistical analysis can be found in Supplementary Table S15. **B,** Representative pictures of infected leaves at 12 dpi are shown.

UMAG_00054, *UMAG_05780*, and *UMAG_06223* (Schilling et al. 2014; Supplementary Fig. S1C).

To link the reduced virulence observed in mutants lacking *UMAG_00054*, *UMAG_00104*, *UMAG_05780*, *UMAG_05932*, *UMAG_11062*, *UMAG_11362*, or *UMAG_11205* with the deletion of the respective gene, complementation strains were created. A complementation strain was also generated for *UMAG_06223*, which was previously implicated in virulence and filamentous growth (Schilling et al. 2014). All complementation strains were made by reintegrating the respective wild-type gene as a single copy into the *ip* locus of the corresponding single mutant strain. Subsequently, the restoration of virulence and filamentation was tested. For six of the eight strains, complementation was successful (Supplementary Fig. S2). *UMAG_00054* only partially complemented the deletion phenotype (Supplementary Fig. S2). In constructs introduced in the mutant for complementation, the wild-type gene is usually cloned with an upstream sequence extending up to the neighboring gene. However, for *UMAG_00054*, this upstream region comprises only 328 base pairs. As previously reported previously for *ros1* (Tollot et al. 2016), we consider that this region may not have included all upstream sequences necessary for full expression of the reintroduced gene and complete complementation. In support, three independently generated *UMAG_00054* mutants showed consistent reduction in virulence, entailing *UMAG_00054* in the disease phenotype. *UMAG_06223* was unable to complement the virulence defect of the respective deletion mutant (Schilling et al. 2014). As we only had a single published mutant for *UMAG_06223*, we regenerated three independent *UMAG_06223* mutant strains and examined their vegetative growth and virulence phenotypes in an attempt to explain the failure in complementation. All three mutants were indistinguishable from the parental strain SG200 (Supplementary Fig. S3). This shows that the virulence defect seen in the original *UMAG_06223* mutant (Schilling et al. 2014; Fig. 2) is caused by a spontaneous mutation not linked to the gene. Thus, 20 of the 53 core effector groups defined here contribute to virulence.

Analyzing the expression patterns, sequence, and structural properties of effectors that contribute to virulence

To gain insights into the characteristics of the effectors that contribute to virulence, we retrieved the expression profiles of each effector during disease progression (Lanver et al. 2018). We then compared the expression profiles of core effectors, non-core effectors (i.e., accessory), and those core novel effectors with and without virulence contribution. We found discrete differences among the expression patterns of these groups. Core effectors have higher mean expression in early stages in comparison to accessory ones (Fig. 3A). Novel core effectors are expressed more at 2, 4, and 6 dpi in comparison to the rest (Fig. 3B). In addition, novel core effectors that contribute to virulence have a higher mean expression at 1 and 2 dpi in comparison to those novel core effectors that do not contribute to virulence (Fig. 3C). Taking a closer look at the expression profiles of each novel core effector, it is apparent that most of the effectors with a virulence phenotype belong to the magenta module. The magenta module is the one associated with establishment of biotrophy where co-expressed genes are strongly induced from 0.5 to 2 dpi, and the high expression levels are maintained until 12 dpi (Lanver et al. 2018; Fig. 3D).

The sequences of the effectors that contribute to virulence vary in length and have no InterPro-predicted functional domains beside regions predicted to be disordered, which adopt many conformations or stay unfolded (Fig. 4A; Supplementary Table S11). To gain insights into the structural properties of these effectors, we modeled the structures of all *U. maydis* effectors from the 53 homologous groups using ColabFold v.1.5.3 (Mirdita et al. 2022) that relies on AlphaFold v.2.3.2 (Jumper et al. 2021). About 40% of the models showed predicted template modeling (pTM) scores smaller than 0.5, indicating low accuracy (Fig. 4; Supplementary Table S5). This could partially be attributed to the presence of intrinsically disordered regions in many effectors, as they do not adopt a single foldable conformation (Fig. 4A). We found no obvious structural similarities among the effectors essential for virulence when the entire structures were compared (Fig. 4B). However, well-folded regions of Pep1 and Stp3 displayed some domain-level structural similarity, although the implication of this resemblance to their functions is unknown. Among the effectors contributing to virulence, UMAG_05932 stands out, as it contains the Tin2-like fold (Seong and Krasileva 2023; Fig. 4C).

Assessing the presence of homologs of core effectors without any apparent contribution to virulence

Mutants in 33 effector groups showed no changes in virulence in comparison to the parental strain (Fig. 2; Supplementary Table S4). An explanation for the lack of virulence for these strains could be the presence of one or more sequence-divergent or structural homologs with functional redundancy to the deleted genes, which we might have missed in our sequence-based searches. To assess this, we used Foldseek to search for structural homologs of these proteins among the *U. maydis* proteome and built corresponding clusters of structurally similar proteins. When comparing the 33 effector groups with the structural clusters, we found the grouping to be identical in 20 cases, most of them singletons (Supplementary Table S4).

For the remaining 13 groups, the structural clusters had at least one additional member compared with our initial grouping. In three cases (clusters 2, 7, and 16) members of distinct homologous groups were clustered based on their structural similarity (Supplementary Table S4). Structural cluster 16 stands out, as it comprises UMAG_05227 and UMAG_05604, which were singleton based on sequence-derived clustering but well superimposed based on structures (Fig. 5A). If the additional structural homologs provide functional redundancy, they could have functionally substituted for the deleted genes and could have masked virulence phenotypes. Simultaneous deletion of these homologs will be needed in future to evaluate this possibility.

It is worth noting that some structural clusters contain effectors that do and do not contribute to virulence. Structural cluster number 2 includes seven members of the Eff1 family (Khrunyk et al. 2010) along effectors that do not contribute to virulence. Structural cluster number 5 connects both members of the Eff3 family (no contribution to virulence) with UMAG_05932 (contribution to virulence) (Supplementary Table S4). Superimposition of the structure of UMAG_05932 with those of the Eff3 effectors support their similarity, assigning them to the previously identified Tin2-like SUSS effector family (Fig. 5B; Seong and Krasileva 2023). If this clustering based on predicted structures indicates functional redundancy, we could expect a stronger virulence phenotype upon co-deletion of the respective genes.

Discussion

Studying the mechanisms pathogens use to cause disease has proven to be a powerful strategy to understand plant immunity and generate solutions for agriculture. Effector proteins are the key pathogen molecules that promote disease progression. To boost the identification of promising effector proteins for functional characterization, we pursued the hypothesis that conserved secreted proteins without known domains might be critical to pathogen virulence, forming a functional group. To do so, we defined homologous groups of novel secreted proteins from 11

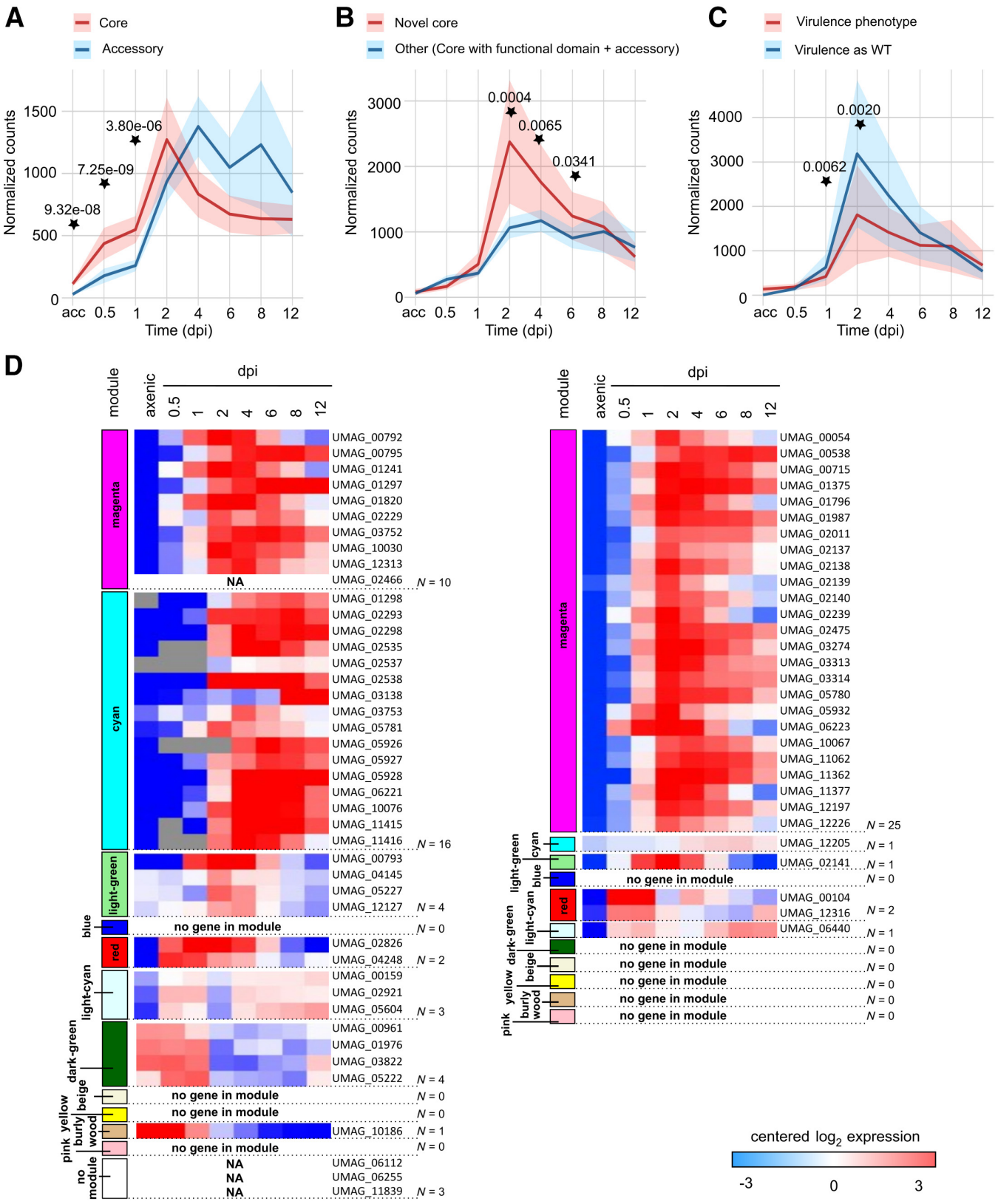

Fig. 3. Analysis of the expression patterns of *Ustilago maydis* effectors. Line bars depicting the mean expression of the selected groups of genes during *U. maydis* infection. **A,** Core effectors versus accessory, **B,** novel core effectors versus non-novel core effectors (core effectors with functional domain and accessory effectors), and **C,** novel core effectors not contributing to virulence versus novel core effectors contributing to virulence phenotype. Stars mark the time points at which the gene groups compared present a significant difference in the mean expression according to Wilcoxon rank-sum test with Bonferroni correction for multiple testing. Confidence zones correspond to the standard error. **D,** Heat maps show expression of genes encoding novel core effectors not contributing to virulence (left) and contributing to virulence (right). Modules as defined by Lanver et al. (2018) are indicated on the left, and the number of effectors in the corresponding module on the right. dpi, days postinfection.

pathogenic species in the Ustilaginaceae family. This comparative genomics approach allowed the identification of 53 core effector candidate groups. To test whether these proteins have a role in virulence, we obtained or generated *U. maydis* mutant strains by knocking out a single gene or the whole gene family of the core groups. We then quantified the severity of the disease caused by each mutant strain in maize seedling infections and compared it with the one caused by the parental strain.

Of the 53 mutant strains, 20 showed reduced virulence compared with the control. Among these, 18 were single mutants, and 2 were gene family mutants. Among the group of effectors that contribute to virulence, those reported to participate in the formation of a cell surface-exposed effector complex (Ludwig et al. 2021) are the only ones (except for *pit1*) for which deletion completely abolishes virulence. This might reflect the fact that these proteins likely have an early structural function as complex building blocks besides having a potential effector function as described for Pep1, for instance, which also acts as a peroxidase inhibitor (Doehlemann et al. 2009). When the structures of these proteins were modeled, no distinctive structural motives or obvious similarities were found (Fig. 4B). This suggests that the building blocks of the effector complex are heterogeneous in structure. In our study, the *pit2* mutant also showed no virulence symptoms, while weak symptoms were observed in another study (Doehlemann et al. 2011). This difference could be caused by the plant variety used for the infections or by dif-

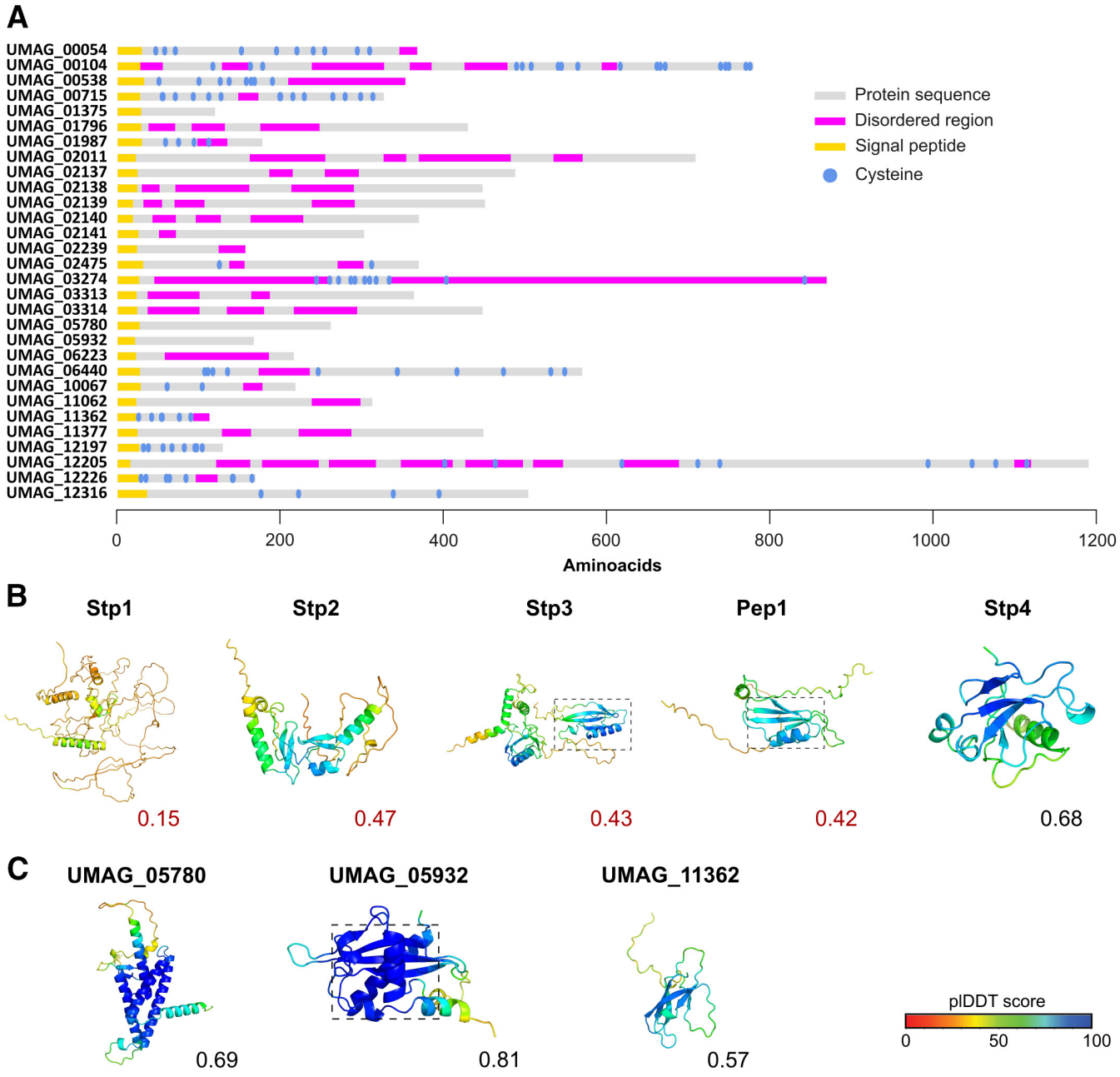

Fig. 4. Sequence and structural properties of novel effectors contributing to virulence. **A,** Schematics of the sequence features of the effectors contributing to virulence. Amino acid sequences of effectors are drawn to scale. **B and C,** Best structures predicted by AlphaFold for selected *Ustilago maydis* effectors that contribute to virulence with their predicted template modeling (pTM) scores ranging from 0 (worst) to 1 (best). Models are colored using a rainbow scheme based on their predicted local distance difference test (pLDDT) scores, which range from 0 (worst) to 100 (best). **B,** Effectors that are essential for virulence. The boxes highlight the similar region between Stp3 and Pep1. **C,** Effectors contributing to virulence. The box highlights the Tin2-like effector fold (Seong and Krasileva 2023).

ferences in the glasshouse settings. *pit2* mutants are able to proliferate comparably to SG200 in the infected tissue up to 2 dpi (Doehlemann et al. 2011), while mutants lacking members of the surface complex (Stp complex) do not proliferate and become growth-arrested earlier in the epidermal layer (Ludwig et al. 2021). Therefore, Pit2 is clearly less essential for virulence than the seven proteins forming the Stp complex. Among the 20 strains with a virulence phenotype, 13 had been previously reported in various studies published between 2010 and 2021 (Supplementary Table S4). Here we followed the hypothesis that conserved secreted proteins without known domains present a rich source of effectors contributing to virulence. In fact, in this work only, we report seven new interesting bona fide effector candidates for functional characterization.

To assess whether the common presence of bona fide effectors across smut species translates to functional conservation, additional assays are needed. To date, cross-complementation analyses have been done for eight of the previously characterized novel core effectors. Cross-species complementation assays for *pep1*, *stp1*, and *stp4* showed that these are functionally conserved (Seitner et al. 2018; Sharma et al. 2019), suggesting that the protein complex formed by these seven effectors may be functional in other smuts (Ludwig et al. 2021). Similarly, the virulence phenotype of the *sta1* deletion mutant in *U. maydis* could be complemented by introducing orthologs from four smut species (Tanaka et al. 2020), and the *U. maydis rsp3* deletion mutant could be complemented by the *S. reilianum* f. sp. *zeae rsp3* ortholog (Ma et al. 2018). In contrast, the *U. hordei* ortholog of *see1* did not complement the *U. maydis see1* deletion strain (Redkar et al. 2015a), and the *pit2* orthologs from *U. hordei*, *S. reilianum* f. sp. *zeae*, and *M. pennsylvanicum* did not complement the *U. maydis pit2* deletion strain (Misas Villamil et al. 2019). Furthermore, the *S. reilianum* f. sp. *zeae tin2* ortholog not only did not complement the *U. maydis tin2* deletion strain but was shown to have a distinct function in maize (Tanaka et al. 2019). An intermediate behavior was observed for *apB73*, as the *apB73* deletion strain in *U. maydis* could be complemented by introducing the ortholog from *S. reilianum* f. sp. *zeae* but not those from *U. bromivora* or *M. pennsylvanicum* (Stirnberg and Djamei 2016). These results indicate that belonging to the core group of effectors is no guarantee of functional conservation.

AlphaFold 2 could not accurately predict the structures of many effectors contributing to virulence (Fig. 4C; Supplementary Table S5). Yet our results were consistent with the postulation of the previous study that pathogen effectors could have originated from ancient nonpathogenic ancestors and evolved divergently for novel functions (Seong and Krasileva 2023). Furthermore, structural similarity searches with Foldseek identified significant matches for UMAG_05780 and UMAG_11362 in *Moesziomyces antarcticus* and *Pseudozyma hubeiensis*, respectively (Fig. 4C; Supplementary Table S5). These species belong to Ustilaginomycetes and are not known to be plant pathogenic but present secretome overlap with pathogenic smut fungi (Schuster et al. 2018). The conservation of these proteins between pathogenic and nonpathogenic species potentially implies that some *U. maydis* proteins have acquired pathogenic functions along evolutionary time.

To date, nine non-core, novel effectors have been identified as potential virulence factors through multiple studies, and only a single gene in this group was reported to have no actual contribution to virulence (Darino et al. 2021; Schilling et al. 2014; Schurack et al. 2021; Zuo et al. 2021, 2023). As mutants without virulence phenotypes are unlikely to be published, this high incidence of mutants with a virulence phenotype might be misleading, because we currently lack a systematic deletion study of novel, non-core effectors. Therefore, we cannot currently assess whether our focus on novel core effectors has particularly increased the chances of detecting effectors with a virulence contribution. Nevertheless, we did successfully find effectors that contribute to virulence among core novel secreted proteins, following our hypothesis about them.

Out of the 53 groups identified, 33 deletion mutants did not show a virulence phenotype under the tested conditions. For 13 of these genes, further analysis revealed the presence of structural homologs, which might have functional redundancy. Evaluating this possibility will require generation of multigene knockouts and additional phenotyping. For the remaining 20 of these 33, we could not identify other structurally similar effectors within *U. maydis* and were unable to link the lack of a virulence defect with functional overlap between evolutionarily related proteins. The lack of phenotype could be attributed to our phenotyping method. We have tested virulence via disease severity quantification using macroscopic symptoms of seedling infections in greenhouse conditions. This excludes effects on older plants, symptoms in male and female flowers, and the microbiome, among others (Depotter et al. 2021). Moreover, deletion mutants were generated in the solopathogenic strain SG200, in which the contribution of effectors to spore formation cannot be reliably assessed (Fukada et al. 2021). Another possibility is the presence of evolutionarily unrelated effectors that may have functionally converged. Our strategy to identify and target homologous groups would miss such effectors. Despite these potential shortcomings, our focus on core effectors has awarded us with a high number of mutants affected in virulence and with new bona fide effectors for functional characterization.

Materials and Methods

Strains and growth conditions

The *Escherichia coli* strain Top10 (Life Technologies) was used for cloning purposes. *U. maydis* strains used in this study are listed in Supplementary Table S5. They are derived from the solopathogenic strain SG200 (Kämper et al. 2006).

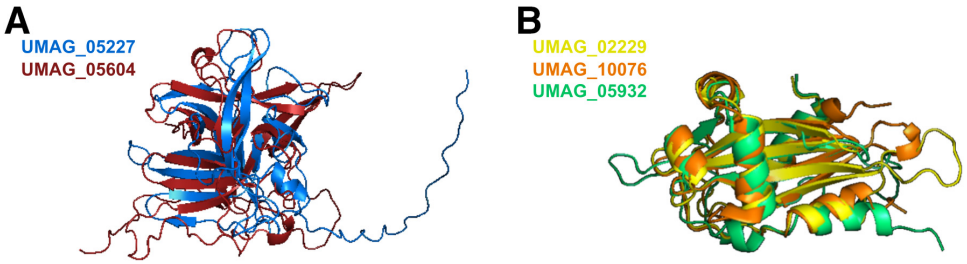

Fig. 5. Novel core effectors displaying similar structures could show functional redundancy. Best structures predicted by AlphaFold for selected *Ustilago maydis* effectors were superimposed in PyMOL. **A,** Structural cluster 16 contains two sequence-unrelated effectors. **B,** Structural cluster 5 contains *U. maydis* proteins displaying the Tin2-like fold, including members of the Eff3 family (no virulence contribution) and UMAG_05932, an effector contributing to virulence.

U. maydis strains were grown in liquid YEPSL (0.4% yeast extract, 0.4% peptone, 2% sucrose) at 28°C on a rotary shaker at 200 rpm. Colony morphology was assessed by propagating the strains to an OD_{600} of 1.0 in YEPSL and spotting 2.5 µl on PD plates (BD-Difco potato dextrose medium, 2% agar). PD plates were incubated for 48 h at 28°C, and colony morphology was assessed relative to SG200. Growth was assessed by streaking out strains on PD plates and comparing the size of single colonies of the mutant relative to SG200 after 48 h at 28°C. To assess filamentation, *U. maydis* strains were grown to an OD_{600} of 1.0 in YEPSL, and 2.5 µl was spotted on PD charcoal (PD supplemented with 1% activated charcoal). Plates were sealed with Parafilm and incubated for 48 h at room temperature.

Strain constructions and verification

Deletion strains provided by other groups are listed in Supplementary Table S6. The deletion events in these strains were confirmed via Southern blot analysis. Deletion strains generated in this study and the gene modification strategy used are listed in Supplementary Table S6. Deletion strains were either generated by gene replacement via double homologous recombination following the previously described PCR-based method (Kämper 2004) or CRISPR-Cas9-mediated gene disruption of single or multiple genes (Schuster et al. 2016, 2018). For the scarless deletion of clustered genes, CRISPR-Cas9 was used in conjunction with donor DNA. To this end, single guide RNAs (sgRNAs) targeting one of the clustered genes were designed using the online tool E-CRISP (Heigwer et al. 2014). The best hit was chosen regardless of its position in the gene. Oligonucleotides encoding sgRNA templates were cloned in Acc65I-linearized pMS73 (Schuster et al. 2018) via Gibson assembly (Gibson et al. 2010). Donor DNAs ranging from 40 to 100 bp in length and comprising the up- and downstream flanking sequences of the gene cluster to be deleted were synthetized as oligonucleotides (Eurofins). CRISPR plasmids (no more than 0.5 µg) and donor DNAs (1 µg) were co-transformed in *U. maydis*, as described before (Schulz et al. 1990). Precise editing was confirmed by PCR and Southern blot analysis.

For complementation of *U. maydis* deletion mutants, genes including native promoter and terminator sequences were cloned in the integrative p123 plasmid (Aichinger et al. 2003) containing an *ip* allele that confers carboxin resistance (Keon et al. 1991). The p123-derived plasmids were linearized as indicated in Supplementary Table S2 before transformation in *U. maydis*. Linearized constructs were integrated single copies into the genomes of effector mutant strains carrying a carboxin sensitive *ip* allele via homologous recombination (Loubradou et al. 2001). The complementation strains were verified by Southern blot analysis.

Resequencing of *M. pennsylvanicum* strain Mp4, genome assembly, and annotation

As the genome sequence of *M. pennsylvanicum* Mp4 derived by Illumina sequencing (Sharma et al. 2014) did not allow detecting all essential effectors (Ludwig et al. 2021), we improved the genome quality by resequencing *M. pennsylvanicum* Mp4 by single-molecule real-time sequencing (SMRT). DNA was isolated using a phenol-based protocol (Hoffman and Winston 1987). A single large insert library (15 to 20 kb) was constructed at the Max Planck Genome Centre in Cologne and sequenced in one cell using P5-C3 chemistry on the PacBio RS II (Pacific Biosciences) sequencing platform. This yielded 212,236 reads with an average length of 11,464 bp, corresponding to an average 121.8-fold coverage.

A de novo assembly was done using the program HGAP2 with the BLASR aligner version 1 from SMRT analysis. The minimum seed length was 6,000 bp, maximum divergence was set to 30%, and minimum anchor size was 12 bp. Polishing the assembly was done using only unambiguously mapped PacBio reads. Primary structural annotation was achieved by applying three de novo prediction programs: (i) Fgenesh (Salamov and Solovyev 2000) with different matrices (trained on *Aspergillus nidulans*, *Neurospora crassa*, and a mixed matrix based on different species); (ii) GeneMark-ES (Ter-Hovhannisyan et al. 2008); and (iii) AUGUSTUS (Stanke et al. 2006). In addition, the protein sequences of *U. maydis* (Kämper et al. 2006), *U. bromivora* (Rabe et al. 2016), and *S. reilianum* (Schirawski et al. 2010) were mapped on the scaffolds using Exonerate (Slater and Birney 2005). Resulting gene call models were checked for complete mappings. Incomplete mappings were additionally inspected by using multi t-coffee alignments to the orthologous protein sequences of the species mentioned above to improve the correction process of the gene structure in *M. pennsylvanicum*. All gene structures and evidence were displayed in GBrowse (Donlin 2007), allowing manual validation and correction of all coding sequences. The final annotation set comprises 6,868 protein-coding genes. In addition, 286 tRNA-encoding genes were predicted using tRNAscan-SE (Lowe and Eddy 1997). The protein-coding genes were analyzed and functionally annotated using the Pedant system (Walter et al. 2009). The genome sequence and annotation were submitted to the European Nucleotide Archive, ENA at http://www.ebi.ac.uk/ena/data/view/OAPG01000001-OAPG01000063. This new version of the proteome contained 728 proteins that were not annotated in the previous version of the genome by Sharma et al. (2014), among which 57 are predicted to be secreted. Conversely, our annotation lacks 212 proteins that were annotated by Sharma et al. (2014), but none of them is predicted to be secreted (Supplementary Table S7).

Prediction of secreted proteins

Sources of proteome data for the seven smut species investigated in this study are listed in Supplementary Table S1. The proteins of the seven species were filtered with a customized Python script for sequences starting with an N-terminal methionine to ensure that prediction of secretion is only performed with complete protein sequences (https://github.com/gschwei/EDB/blob/main/Data/getCleanProtSequences.py). In this way, 8 proteins in *U. bromivora*, 26 in *U. hordei*, 30 in *U. maydis*, 36 in *S. scitamineum*, 20 in *S. reilianum* f. sp. *zeae*, and 20 in *S. reilianum* f. sp. *reilianum* were excluded from further analyses. The remaining protein sequences were used to predict secretion using SignalP 4.1 with the default Conservative mode (Petersen et al. 2011). Next, transmembrane domains were predicted with version TMHMM 2.0c (Krogh et al. 2001) and Phobius (Käll et al. 2004). Phobius predictions were run with the corresponding online tool (http://phobius.sbc.su.se/index.html) using the options Normal Prediction and output format Short on July 11, 2017. Finally, C-terminal retention motifs for localization to the ER were predicted with the online tool of PS Scans (http://www.hpa-bioinfotools.org.uk/cgi-bin/ps_scan/ps_scanCGI.pl; accessed July 11, 2017). We selected the standard PROSITE pattern "PS00014-ER_TARGET" to identify ER retention signals. This PROSITE pattern considers the consensus sequence [KRHQSA]-[DENQ]-E-L as an ER-retention motif. Proteins were considered to be secreted if (i) SignalP identified a signal peptide, (ii) neither TMHMM nor Phobius predicted a transmembrane domain downstream of the inferred signal peptide cleavage site, and (iii) no ER retention motif could be found. Scripts related to this analysis can be found under: https://github.com/gschwei/EDB.

Building groups of homologous proteins

The secretome of all seven species was used to infer groups of homologous proteins using OrthoMCL (Enright et al. 2002). The result of an all-against-all blastp search (Altschul et al. 1990) was used to obtain alignment scores, and these values were used as pairwise distance measures between sequences for the input to OrthoMCL, which was run in the Label Mode. In this mode, the clustering of proteins depends on setting the inflation value, which determines the composition of resulting groups. To identify an inflation value suitable for our analysis, two criteria had to be met. The value had to be small enough to allow the grouping of previously described effector gene families in *U. maydis*, and it had to be high enough to avoid the inclusion of unrelated sequences. The effector gene families used as readout comprised the *Eff1* family (Khrunyk et al. 2010), the "brown," "green," and *Tin1* gene families of the effector gene cluster 19A (Brefort et al. 2014), the *Mig1* and *Mig2* gene families (Basse et al. 2002; Schirawski et al. 2010), and a previously defined family of endoglucanases (Lanver et al. 2014; Supplementary Table S8). We tested a range of inflation values from 1.0 to 1.6, and found that an inflation value of 1.5455 allowed the correct detection of most reference families without additional paralogs, except *UMAG_02135* and *UMAG_02136*, the most distant members of the *Eff1* family (Khrunyk et al. 2010; Supplementary Table S9). When using this value for building groups of homologs, we obtained 398 groups of homologous protein sequences predicted to be secreted (Supplementary Table S10). Scripts related to this analysis can be found under: https://github.com/gschwei/EDB.

Prediction of protein domains

InterProScan (v.5.25-64.0) combining 16 prediction software programs (Finn et al. 2017) was employed in stand-alone mode on Linux to infer domains in all predicted secreted proteins (Supplementary Table S11). All domain predictions present in the groups of homologs were manually screened and sorted either as "functional domain" or "not a functional domain" (Supplementary Table S12). Based on this classification, homologous groups were sorted into three categories: all members with functional domains, all members without functional domains, and a mix of members with and without functional domains. The members in each mixed homologous group were aligned using PRANK v.100802 with default settings (Löytynoja and Goldman 2008). Each alignment was manually investigated, and each mixed homologous group was resorted into either the category "all proteins with functional domain" or the category "all proteins without functional domain." In some cases, the alignment revealed that groups contained sequences incorrectly classified as homologous. In these cases, the groups were manually curated following alignment information and subsequently split into subgroups.

Modifications introduced after manual curation and their justifications are summarized in Supplementary Table S13 and Supplementary Fig. S4. After this manual curation, the number of groups increased from 398 to 462, among which 214 belong to the category "with functional domain" and 248 groups are classified as "without functional domain" (Supplementary Table S2). We then mined this curated dataset for groups of homologous proteins containing sequences from all species studied (core sequences). Of the 462 groups, 140 are core groups (86 with functional domain and 53 without functional domains) (Supplementary Table S2). One example of manual curation is Group_150 containing the novel effector Cce1/Stp4 (UMAG_12197) (Ludwig et al. 2021; Seitner et al. 2018). Homologs of Cce1/Stp4 were found in all species but not in *M. pennsylvanicum* (Supplementary Table S7). The blastp searches of Stp4 against the newly annotated resequenced *M. pennsylvanicum* genome detected MEPE_02537 in a region that is syntenic between *U. maydis* and *M. pennsylvanicum* and encodes a protein with 54% identity to *U. maydis* Cce1/Stp4. We identified a D-score of 0.486 for MEPE_02537 with SignalP, which is below the D-score threshold of 0.5 used for predicting secretion. However, given the experimental evidence for Cce1/Stp4 secretion (Ludwig et al. 2021; Seitner et al. 2018), we manually included MEPE_02537 as a homolog of UmStp4 in our data set. The set of novel core effectors is now considered to comprise 53 groups (Fig. 1; Supplementary Table S2). Scripts related to this analysis can be found under: https://github.com/gschwei/EDB.

BLAST search of core effectors in other smuts

To account for potential homologs of core effectors in four published plant-infecting smut fungi genomes (*U. trichophora*, *U. esculenta*, *U. triciti*, and *U. hordei* [Uhor1]), we retrieved secretome data for these species as described earlier. Sources of proteome data for these species are listed in Supplementary Table S1. Homologous genes of novel core effectors were identified by blastp searches with protein sequences of *U. maydis* novel core effectors as the query, and the secretomes of the four additional species as the database. The blastp hits were found for 31 of the 53 groups of core effectors. We reasoned that missing blastp hits could result from false-negative prediction of secretion. Therefore, we repeated the blastp search with *U. maydis* novel core effectors against the entire proteomes of the four species. This new blastp search retrieved 14 hits outside the predicted secretomes. Alignments and manual inspection were then performed to define whether the group remained core or not. For the remaining eight cases where no blastp hit was found, tblastn searches were performed, and the results were manually inspected to decide whether the group remained core. We could find homologs of all 53 *U. maydis* novel core effectors in *U. trichophora*, *U. esculenta*, *U. triciti*, and the strain Uhor1. Details of the manual inspection are summarized in Supplementary Table S14 and Supplementary Figure S5, and the core effectors in 11 smut fungi are listed in Supplementary Table S3. We did not include the proteome of *Thecaphora thlaspeos* (Courville et al. 2019) in this study, because it belongs to the more distant family Glomosporiaceae (Begerow et al. 2014).

Virulence assays

Virulence of the strains was assessed by infecting maize seedlings. Strains were grown in YEPSL medium to an optical density OD_{600} of 0.8 to 1.0. The cells were harvested via centrifugation (1,700 × *g*, 5 min, room temperature) and resuspended in H_2O to a final OD_{600} of 1.0. The suspension was syringe-inoculated into 7-day-old 'Early Golden Bantam' (Urban Farmer) *Zea mays* seedlings grown in a glasshouse as described previously (Kämper et al. 2006). Disease symptoms were evaluated according to reported disease rating criteria (Kämper et al. 2006).

For the mutants we generated in this study, initial virulence assays were made with at least two independently generated strains per mutant and SG200 as the control. If virulence phenotypes were dissimilar between mutant strains (because of mutagenic events during the protoplasting step), and one or more were unaltered in virulence, one of these mutants was selected for further investigation. If all mutants were affected in virulence, one was chosen for complementation.

Once available, all mutants were assayed in parallel using one strain of each core effector mutant and the SG200 control. The number of infected plants used in this assay was predetermined by a sample size estimation performed with the pwr library v.1.2.2 (Champely 2020) in R (v.3.5.1; R Core Team 2018) with the following parameters: $d = 0.80$, sig.level $= 0.01$, power $=$ 0.9. The desired effect size was determined based on previous

infections made with deletion mutants giving either a strong virulence defect like *scp2* mutants (Krombach et al. 2018) or a weak virulence defect like *cmu1* mutants (Djamei et al. 2011).

To detect significant differences, we increased by 15% the sample size obtained ($n = 50$) given that virulence test are non-parametric tests. In practice, 20 plants were infected in parallel with each mutant strain, and the experiment was independently repeated twice. Differences in virulence scores were assessed with a Kruskal-Wallis test (Kruskal and Wallis 1952) followed by a Conover-Iman post hoc test (Conover and Iman 1979) for pairwise comparisons, using the conover.test package v.1.1.5. False discovery rate (FDR) was used as correction for multiple testing (Benjamini and Hochberg 1995) and calculated with the *conover.test* function (using the parameter method ="bh"). Differences in virulence with an FDR < 0.01 were considered as significant. Statistical analysis can be found in Supplementary Table S15.

Structure prediction

We predicted the structures of 73 putative effectors in the 53 homologous groups. The protein sequences without signal peptide were submitted to ColabFold v.1.5.3 (Mirdita et al. 2022) that relies on AlphaFold v.2.3.2 (Jumper et al. 2021). The pTM model was used to generate five models with sequences collected from the standard databases (msa_mode: mmseqs2_uniref_env) and available experimentally determined structures as templates (template_mode: pdb100). The best model was selected based on pLDDT scores and further relaxed with amber. The structure of UMAG_06112 was downloaded from the AlphaFold protein structure database (Varadi et al. 2022). This protein was known to be well predicted by AlphaFold 2, but ColabFold failed to model it.

Structural similarity searches

To identify structural matches outside the smut pathogens included in this study, the best-predicted structure for each protein was submitted to the Foldseek web server to search against the AlphaFold database clustered at 50% sequence identity (AF50) (van Kempen et al. 2024). We reported the best hit that did not originate from *Ustilago*, *Melanopsichium*, and *Sporisorium* (Supplementary Table S4). To identify structural matches within the *U. maydis* proteome, we downloaded the pre-existing 6,347 structural models from the AlphaFold database, using the taxonomical identifier (237631). From each of the models we downloaded and modeled, low-confidence N- and C-terminal regions were removed based on pLDDT < 40. If the average pLDDT score of the remaining positions exceeded 60, and the remaining protein was equal to or longer than 50 amino acids, the model was included for structural clustering. The selection criterion chosen was lower than the standard (pLDDT > 70) to identify any potential matches that AlphaFold 2 may not model well. All models were clustered with Foldseek v.1cb3a80d9566820bc223bdf4d34d30d85ffbc4f4 (easy-cluster -s 7.6 -c 0.7).

Acknowledgments

We are grateful to the many colleagues who provided mutant strains. We thank Marco Thines for providing the Mp4B *M. pennsylvanicum* strain.

Literature Cited

Agrios, G. N. 2005. Plant Pathology, 5th Edition. Elsevier, Amsterdam, the Netherlands.

Aichinger, C., Hansson, K., Eichhorn, H., Lessing, F., Mannhaupt, G., Mewes, W., and Kahmann, R. 2003. Identification of plant-regulated genes in *Ustilago maydis* by enhancer-trapping mutagenesis. Mol. Genet. Genomics 270:303-314.

Altschul, S. F., Gish, W., Miller, W., Myers, E. W., and Lipman, D. J. 1990. Basic local alignment search tool. J. Mol. Biol. 215:403-410.

Basse, C. W., Kolb, S., and Kahmann, R. 2002. A maize-specifically expressed gene cluster in *Ustilago maydis*. Mol. Microbiol. 43: 75-93.

Begerow, D., Bauer, R., and Boekhout, T. 2000. Phylogenetic placements of ustilaginomycetous anamorphs as deduced from nuclear LSU rDNA sequences. Mycol. Res. 104:53-60.

Begerow, D., Schäfer, A. M., Kellner, R., Yurkov, A., Kemler, M., Oberwinkler, F., and Bauer, R. 2014. Ustilaginomycotina. Pages 295-329 in: The Mycota: Systematics and Evolution. D. J. McLaughlin and J. W. Spatafora, eds. Springer, Berlin, Germany.

Begerow, D., Stoll, M., and Bauer, R. 2006. A phylogenetic hypothesis of Ustilaginomycotina based on multiple gene analyses and morphological data. Mycologia 98:906-916.

Benevenuto, J., Teixeira-Silva, N. S., Kuramae, E. E., Croll, D., and Monteiro-Vitorello, C. B. 2018. Comparative genomics of smut pathogens: Insights from orphans and positively selected genes into host specialization. Front. Microbiol. 9:660.

Benjamini, Y., and Hochberg, Y. 1995. Controlling the false discovery rate: A practical and powerful approach to multiple testing. J. R. Stat. Soc.: Ser. B (Methodol.) 57:289-300.

Bindics, J., Khan, M., Uhse, S., Kogelmann, B., Baggely, L., Reumann, D., Ingole, K. D., Stirnberg, A., Rybecky, A., Darino, M., Navarrete, F., Doehlemann, G., and Djamei, A. 2022. Many ways to TOPLESS–manipulation of plant auxin signalling by a cluster of fungal effectors. New Phytol. 236:1455-1470.

Borah, N., Albarouki, E., and Schirawski, J. 2018. Comparative methods for molecular determination of host-specificity factors in plant-pathogenic fungi. Int. J. Mol. Sci. 19:863.

Brefort, T., Tanaka, S., Neidig, N., Doehlemann, G., Vincon, V., and Kahmann, R. 2014. Characterization of the largest effector gene cluster of *Ustilago maydis*. PLoS Pathog. 10:e1003866.

Champely, S. 2020. pwr: Basic functions for power analysis. R package. https://cran.r-project.org/web/packages/pwr/index.html (accessed December 2020).

Conover, W. J., and Iman, R. L. 1979. Multiple-Comparisons Procedures. Informal Report. Los Alamos National Lab, Los Alamos, NM.

Courville, K. J., Frantzeskakis, L., Gul, S., Haeger, N., Kellner, R., Heßler, N., Day, B., Usadel, B., Gupta, Y. K., van Esse, H. P., Brachmann, A., Kemen, E., Feldbrügge, M., and Göhre, V. 2019. Smut infection of perennial hosts: The genome and the transcriptome of the Brassicaceae smut fungus *Thecaphora thlaspeos* reveal functionally conserved and novel effectors. New Phytol. 222:1474-1492.

Darino, M., Chia, K.-S., Marques, J., Aleksza, D., Soto-Jiménez, L. M., Saado, I., Uhse, S., Borg, M., Betz, R., Bindics, J., Zienkiewicz, K., Feussner, I., Petit-Houdenot, Y., and Djamei, A. 2021. *Ustilago maydis* effector Jsi1 interacts with Topless corepressor, hijacking plant jasmonate/ethylene signaling. New Phytol. 229:3393-3407.

Depotter, J. R. L., and Doehlemann, G. 2020. Target the core: Durable plant resistance against filamentous plant pathogens through effector recognition. Pest Manag. Sci. 76:426-431.

Depotter, J. R. L., Zuo, W., Hansen, M., Zhang, B., Xu, M., and Doehlemann, G. 2021. Effectors with different gears: Divergence of *Ustilago maydis* effector genes is associated with their temporal expression pattern during plant infection. J. Fungi 7:16.

Djamei, A., Schipper, K., Rabe, F., Ghosh, A., Vincon, V., Kahnt, J., Osorio, S., Tohge, T., Fernie, A. R., Feussner, I., Feussner, K., Meinicke, P., Stierhof, Y.-D., Schwarz, H., Macek, B., Mann, M., and Kahmann, R. 2011. Metabolic priming by a secreted fungal effector. Nature 478: 395-398.

Doehlemann, G., Reissmann, S., Aßmann, D., Fleckenstein, M., and Kahmann, R. 2011. Two linked genes encoding a secreted effector and a membrane protein are essential for *Ustilago maydis*-induced tumour formation. Mol. Microbiol. 81:751-766.

Doehlemann, G., van der Linde, K., Aßmann, D., Schwammbach, D., Hof, A., Mohanty, A., Jackson, D., and Kahmann, R. 2009. Pep1, a secreted effector protein of *Ustilago maydis*, is required for successful invasion of plant cells. PLoS Pathog. 5:e1000290.

Donlin, M. J. 2007. Using the Generic Genome Browser (GBrowse). Curr. Protoc. Bioinformatics 17:9.9.1-9.9.24.

Dutheil, J. Y., Mannhaupt, G., Schweizer, G., Sieber, C. M. K., Münsterkötter, M., Güldener, U., Schirawski, J., and Kahmann, R. 2016. A tale of genome compartmentalization: The evolution of virulence clusters in smut fungi. Genome Biol. Evol. 8:681-704.

Enright, A. J., Van Dongen, S., and Ouzounis, C. A. 2002. An efficient algorithm for large-scale detection of protein families. Nucleic Acids Res. 30:1575-1584.

Finn, R. D., Attwood, T. K., Babbitt, P. C., Bateman, A., Bork, P., Bridge, A. J., Chang, H.-Y., Dosztányi, Z., El-Gebali, S., Fraser, M., Gough, J., Haft, D., Holliday, G. L., Huang, H., Huang, X., Letunic, I., Lopez, R., Lu, S., Marchler-Bauer, A., Mi, H., Mistry, J., Natale, D. A., Necci, M., Nuka, G., Orengo, C. A., Park, Y., Pesseat, S., Piovesan, D., Potter, S. C., Rawlings, N. D., Redaschi, N., Richardson, L., Rivoire, C., Sangrador-Vegas, A., Sigrist, C., Sillitoe, I., Smithers, B., Squizzato, S., Sutton, G., Thanki, N., Thomas, P. D., Tosatto, S. C. E., Wu, C. H., Xenarios, I., Yeh, L.-S., Young, S.-Y., and Mitchell, A. L. 2017. InterPro in 2017—beyond protein family and domain annotations. Nucleic Acids Res. 45:D190-D199.

Fisher, M. C., Gurr, S. J., Cuomo, C. A., Blehert, D. S., Jin, H., Stukenbrock, E. H., Stajich, J. E., Kahmann, R., Boone, C., Denning, D. W., Gow, N. A. R., Klein, B. S., Kronstad, J. W., Sheppard, D. C., Taylor, J. W., Wright, G. D., Heitman, J., Casadevall, A., and Cowen, L. E. 2020. Threats posed by the fungal kingdom to humans, wildlife, and agriculture. mBio 11:e00449-20.

Fukada, F., Rössel, N., Münch, K., Glatter, T., and Kahmann, R. 2021. A small *Ustilago maydis* effector acts as a novel adhesin for hyphal aggregation in plant tumors. New Phytol. 231:416-431.

Gibson, D. G., Smith, H. O., Hutchison, C. A., III, Venter, J. C., and Merryman, C. 2010. Chemical synthesis of the mouse mitochondrial genome. Nat. Methods 7:901-903.

Han, X., Altegoer, F., Steinchen, W., Binnebesel, L., Schuhmacher, J., Glatter, T., Giammarinaro, P. I., Djamei, A., Rensing, S. A., Reissmann, S., Kahmann, R., and Bange, G. 2019. A kiwellin disarms the metabolic activity of a secreted fungal virulence factor. Nature 565:650-653.

Heigwer, F., Kerr, G., and Boutros, M. 2014. E-CRISP: Fast CRISPR target site identification. Nat. Methods 11:122-123.

Hemetsberger, C., Herrberger, C., Zechmann, B., Hillmer, M., and Doehlemann, G. 2012. The *Ustilago maydis* effector Pep1 suppresses plant immunity by inhibition of host peroxidase activity. PLoS Pathog. 8:e1002684.

Hoang, C. V., Bhaskar, C. K., and Ma, L.-S. 2021. A novel core effector Vp1 promotes fungal colonization and virulence of *Ustilago maydis*. J. Fungi 7:589.

Hoffman, C. S., and Winston, F. 1987. A ten-minute DNA preparation from yeast efficiently releases autonomous plasmids for transformation of *Escherichia coli*. Gene 57:267-272.

Huang, L., Ökmen, B., Stolze, S. C., Kastl, M., Khan, M., Hilbig, D., Nakagami, H., Djamei, A., and Doehlemann, G. 2024. The fungal pathogen *Ustilago maydis* targets the maize corepressor *RELK2* to modulate host transcription for tumorigenesis. New Phytol. 241:1747-1762.

Jaswal, R., Kiran, K., Rajarammohan, S., Dubey, H., Singh, P. K., Sharma, Y., Deshmukh, R., Sonah, H., Gupta, N., and Sharma, T. R. 2020. Effector biology of biotrophic plant fungal pathogens: Current advances and future prospects. Microbiol. Res. 241:126567.

Jumper, J., Evans, R., Pritzel, A., Green, T., Figurnov, M., Ronneberger, O., Tunyasuvunakool, K., Bates, R., Žídek, A., Potapenko, A., Bridgland, A., Meyer, C., Kohl, S. A. A., Ballard, A. J., Cowie, A., Romera-Paredes, B., Nikolov, S., Jain, R., Adler, J., Back, T., Petersen, S., Reiman, D., Clancy, E., Zielinski, M., Steinegger, M., Pacholska, M., Berghammer, T., Bodenstein, S., Silver, D., Vinyals, O., Senior, A. W., Kavukcuoglu, K., Kohli, P., and Hassabis, D. 2021. Highly accurate protein structure prediction with AlphaFold. Nature 596:583-589.

Käll, L., Krogh, A., and Sonnhammer, E. L. L. 2004. A combined transmembrane topology and signal peptide prediction method. J. Mol. Biol. 338:1027-1036.

Kämper, J. 2004. A PCR-based system for highly efficient generation of gene replacement mutants in *Ustilago maydis*. Mol. Genet. Genomics 271:103-110.

Kämper, J., Kahmann, R., Bölker, M., Ma, L.-J., Brefort, T., Saville, B. J., Banuett, F., Kronstad, J. W., Gold, S. E., Müller, O., Perlin, M. H., Wösten, H. A., de Vries, R., Ruiz-Herrera, J., Reynaga-Peña, C. G., Snetselaar, K., McCann, M., Pérez-Martín, J., Feldbrügge, M., Basse, C. W., Steinberg, G., Ibeas, J. I., Holloman, W., Guzman, P., Farman, M., Stajich, J. E., Sentandreu, R., González-Prieto, J. M., Kennell, J. C., Molina, L., Schirawski, J., Mendoza-Mendoza, A., Greilinger, D., Münch, K., Rössel, N., Scherer, M., Vraneš, M., Ladendorf, O., Vincon, V., Fuchs, U., Sandrock, B., Meng, S., Ho, E. C. H., Cahill, M. J., Boyce, K. J., Klose, J., Klosterman, S. J., Deelstra, H. J., Ortiz-Castellanos, L., Li, W., Sanchez-Alonso, P., Schreier, P. H., Häuser-Hahn, I., Vaupel, M., Koopmann, E., Friedrich, G., Voss, H., Schlüter, T., Margolis, J., Platt, D., Swimmer, C., Gnirke, A., Chen, F., Vysotskaia, V., Mannhaupt, G., Güldener, U., Münsterkötter, M., Haase, D., Oesterheld, M., Mewes, H.-W., Mauceli, E. W., DeCaprio, D., Wade, C. M., Butler, J., Young, S., Jaffe, D. B., Calvo, S., Nusbaum, C., Galagan, J., and Birren, B. W. 2006. Insights from the genome of the biotrophic fungal plant pathogen *Ustilago maydis*. Nature 444:97-101.

Keon, J. P. R., White, G. A., and Hargreaves, J. A. 1991. Isolation, characterization and sequence of a gene conferring resistance to the systemic fungicide carboxin from the maize smut pathogen, *Ustilago maydis*. Curr. Genet. 19:475-481.

Khan, M., Seto, D., Subramaniam, R., and Desveaux , D. 2018. Oh, the places they'll go! A survey of phytopathogen effectors and their host targets. Plant J. 93:651-663.

Khan, M., Uhse, S., Bindics, J., Kogelmann, B., Nagarajan, N., Ingole, K. D., and Djamei, A. 2023. Tip of the iceberg? Three novel TOPLESS interacting effectors of the gall-inducing fungus *Ustilago maydis*. bioRxiv https://doi.org/10.1101/2023.06.12.544640

Khrunyk, Y., Münch, K., Schipper, K., Lupas, A. N., and Kahmann, R. 2010. The use of FLP-mediated recombination for the functional analysis of an effector gene family in the biotrophic smut fungus *Ustilago maydis*. New Phytol. 187:957-968.

Krogh, A., Larsson, B., von Heijne, G., and Sonnhammer, E. L. L. 2001. Predicting transmembrane protein topology with a hidden Markov model: Application to complete genomes. J. Mol. Biol. 305:567-580.

Krombach, S., Reissmann, S., Kreibich, S., Bochen, F., and Kahmann, R. 2018. Virulence function of the *Ustilago maydis* sterol carrier protein 2. New Phytol. 220:553-566.

Kruskal, W. H., and Wallis, W. A. 1952. Use of ranks in one-criterion variance analysis. J. Am. Stat. Assoc. 47:583-621.

Lanver, D., Berndt, P., Tollot, M., Naik, V., Vranes, M., Warmann, T., Münch, K., Rössel, N., and Kahmann, R. 2014. Plant surface cues prime *Ustilago maydis* for biotrophic development. PLoS Pathog. 10:e1004272.

Lanver, D., Müller, A. N., Happel, P., Schweizer, G., Haas, F. B., Franitza, M., Pellegrin, C., Reissmann, S., Altmüller, J., Rensing, S. A., and Kahmann, R. 2018. The biotrophic development of *Ustilago maydis* studied by RNA-Seq analysis. Plant Cell 30:300-323.

Lanver, D., Tollot, M., Schweizer, G., Lo Presti, L., Reissmann, S., Ma, L.-S., Schuster, M., Tanaka, S., Liang, L., Ludwig, N., and Kahmann, R. 2017. *Ustilago maydis* effectors and their impact on virulence. Nat. Rev. Microbiol. 15:409-421.

Laurie, J. D., Ali, S., Linning, R., Mannhaupt, G., Wong, P., Güldener, U., Münsterkötter, M., Moore, R., Kahmann, R., Bakkeren, G., and Schirawski, J. 2012. Genome comparison of barley and maize smut fungi reveals targeted loss of RNA silencing components and species-specific presence of transposable elements. Plant Cell 24:1733-1745.

Lefebvre, F., Joly, D. L., Labbé, C., Teichmann, B., Linning, R., Belzile, F., Bakkeren, G., and Bélanger, R. R. 2013. The transition from a phytopathogenic smut ancestor to an anamorphic biocontrol agent deciphered by comparative whole-genome analysis. Plant Cell 25:1946-1959.

Lin, Y.-H., Xu, M.-Y., Hsu, C.-C., Damei, F. A., Lee, H.-C., Tsai, W.-L., Hoang, C. V., Chiang, Y.-R., and Ma, L.-S. 2023. *Ustilago maydis* PR-1-like protein has evolved two distinct domains for dual virulence activities. Nat. Commun. 14:5755.

Liu, L., Xu, L., Jia, Q., Pan, R., Oelmüller, R., Zhang, W., and Wu, C. 2019. Arms race: Diverse effector proteins with conserved motifs. Plant Signal. Behav. 14:1557008.

Lo Presti, L., and Kahmann, R. 2017. How filamentous plant pathogen effectors are translocated to host cells. Curr. Opin. Plant Biol. 38:19-24.

Lo Presti, L., Lanver, D., Schweizer, G., Tanaka, S., Liang, L., Tollot, M., Zuccaro, A., Reissmann, S., and Kahmann, R. 2015. Fungal effectors and plant susceptibility. Annu. Rev. Plant Biol. 66:513-545.

Lorrain, C., Gonçalves dos Santos, K. C., Germain, H., Hecker, A., and Duplessis, S. 2019. Advances in understanding obligate biotrophy in rust fungi. New Phytol. 222:1190-1206.

Loubradou, G., Brachmann, A., Feldbrügge, M., and Kahmann, R. 2001. A homologue of the transcriptional repressor Ssn6p antagonizes cAMP signalling in *Ustilago maydis*. Mol. Microbiol. 40:719-730.

Lowe, T. M., and Eddy, S. R. 1997. tRNAscan-SE: A program for improved detection of transfer RNA genes in genomic sequence. Nucleic Acids Res. 25:955-964.

Löytynoja, A., and Goldman, N. 2008. Phylogeny-aware gap placement prevents errors in sequence alignment and evolutionary analysis. Science 320:1632-1635.

Ludwig, N., Reissmann, S., Schipper, K., Gonzalez, C., Assmann, D., Glatter, T., Moretti, M., Ma, L.-S., Rexer, K.-H., Snetselaar, K., and Kahmann, R. 2021. A cell surface-exposed protein complex with an essential virulence function in *Ustilago maydis*. Nat. Microbiol. 6:722-730.

Ma, L.-S., Wang, L., Trippel, C., Mendoza-Mendoza, A., Ullmann, S., Moretti, M., Carsten, A., Kahnt, J., Reissmann, S., Zechmann, B., Bange, G., and Kahmann, R. 2018. The *Ustilago maydis* repetitive effector Rsp3 blocks the antifungal activity of mannose-binding maize proteins. Nat. Commun. 9:1711.

Mirdita, M., Schütze, K., Moriwaki, Y., Heo, L., Ovchinnikov, S., and Steinegger, M. 2022. ColabFold: Making protein folding accessible to all. Nat. Methods 19:679-682.

Misas Villamil, J. C., Mueller, A. N., Demir, F., Meyer, U., Ökmen, B., Schulze Hüynck, J., Breuer, M., Dauben, H., Win, J., Huesgen, P. F., and Doehlemann, G. 2019. A fungal substrate mimicking molecule suppresses plant immunity via an inter-kingdom conserved motif. Nat. Commun. 10:1576.

Mueller, A. N., Ziemann, S., Treitschke, S., Aßmann, D., and Doehlemann, G. 2013. Compatibility in the *Ustilago maydis*-maize interaction requires inhibition of host cysteine proteases by the fungal effector Pit2. PLoS Pathog. 9:e1003177.

Navarrete, F., Gallei, M., Kornienko, A. E., Saado, I., Khan, M., Chia, K.-S., Darino, M. A., Bindics, J., and Djamei, A. 2022. TOPLESS promotes plant immunity by repressing auxin signaling and is targeted by the fungal effector Naked1. Plant Commun. 3:100269.

Navarrete, F., Grujic, N., Stirnberg, A., Saado, I., Aleksza, D., Gallei, M., Adi, H., Alcântara, A., Khan, M., Bindics, J., Trujillo, M., and Djamei, A. 2021. The Pleiades are a cluster of fungal effectors that inhibit host defenses. PLoS Pathog. 17:e1009641.

Ökmen, B., and Doehlemann, G. 2014. Inside plant: Biotrophic strategies to modulate host immunity and metabolism. Curr. Opin. Plant Biol. 20:19-25.

Ökmen, B., Jaeger, E., Schilling, L., Finke, N., Klemd, A., Lee, Y. J., Wemhöner, R., Pauly, M., Neumann, U., and Doehlemann, G. 2022. A conserved enzyme of smut fungi facilitates cell-to-cell extension in the plant bundle sheath. Nat. Commun. 13:6003.

Ökmen, B., Katzy, P., Huang, L., Wemhöner, R., and Doehlemann, G. 2023. A conserved extracellular Ribo1 with broad-spectrum cytotoxic activity enables smut fungi to compete with host-associated bacteria. New Phytol. 240:1976-1989.

Ökmen, B., Kemmerich, B., Hilbig, D., Wemhöner, R., Aschenbroich, J., Perrar, A., Huesgen, P. F., Schipper, K., and Doehlemann, G. 2018. Dual function of a secreted fungalysin metalloprotease in *Ustilago maydis*. New Phytol. 220:249-261.

Ökmen, B., Schwammbach, D., Bakkeren, G., Neumann, U., and Doehlemann, G. 2021. The *Ustilago hordei*–barley interaction is a versatile system for characterization of fungal effectors. J. Fungi 7:86.

Olicón-Hernández, D. R., Araiza-Villanueva, M. G., Pardo, J. P., Aranda, E., and Guerra-Sánchez, G. 2019. New insights of *Ustilago maydis* as yeast model for genetic and biotechnological research: A review. Curr. Microbiol. 76:917-926.

Outram, M. A., Figueroa, M., Sperschneider, J., Williams, S. J., and Dodds, P. N. 2022. Seeing is believing: Exploiting advances in structural biology to understand and engineer plant immunity. Curr. Opin. Plant Biol. 67:102210.

Petersen, T. N., Brunak, S., von Heijne, G., and Nielsen, H. 2011. SignalP 4.0: Discriminating signal peptides from transmembrane regions. Nat. Methods 8:785-786.

Petre, B., and Kamoun, S. 2014. How do filamentous pathogens deliver effector proteins into plant cells? PLoS Biol. 12:e1001801.

R Core Team. 2018. R: A Language and Environment for Statistical Computing. R Foundation for Statistical Computing, Vienna, Austria.

Rabe, F., Bosch, J., Stirnberg, A., Guse, T., Bauer, L., Seitner, D., Rabanal, F. A., Czedik-Eysenberg, A., Uhse, S., Bindics, J., Genenncher, B., Navarrete, F., Kellner, R., Ekker, H., Kumlehn, J., Vogel, J. P., Gordon, S. P., Marcel, T. C., Münsterkötter, M., Walter, M. C., Sieber, C. M., Mannhaupt, G., Güldener, U., Kahmann, R., and Djamei, A. 2016. A complete toolset for the study of *Ustilago bromivora* and *Brachypodium* sp. as a fungal-temperate grass pathosystem. eLife 5:e20522.

Redkar, A., Hoser, R., Schilling, L., Zechmann, B., Krzymowska, M., Walbot, V., and Doehlemann, G. 2015b. A secreted effector protein of *Ustilago maydis* guides maize leaf cells to form tumors. Plant Cell 27:1332-1351.

Redkar, A., Villajuana-Bonequi, M., and Doehlemann, G. 2015a. Conservation of the *Ustilago maydis* effector See1 in related smuts. Plant Signal. Behav. 10:e1086855.

Rovenich, H., Boshoven, J. C., and Thomma, B. P. H. J. 2014. Filamentous pathogen effector functions: Of pathogens, hosts and microbiomes. Curr. Opin. Plant Biol. 20:96-103.

Salamov, A. A., and Solovyev, V. V. 2000. Ab initio gene finding in *Drosophila* genomic DNA. Genome Res. 10:516-522.

Savary, S., Willocquet, L., Pethybridge, S. J., Esker, P., McRoberts, N., and Nelson, A. 2019. The global burden of pathogens and pests on major food crops. Nat. Ecol. Evol. 3:430-439.

Schilling, L., Matei, A., Redkar, A., Walbot, V., and Doehlemann, G. 2014. Virulence of the maize smut *Ustilago maydis* is shaped by organ-specific effectors. Mol. Plant Pathol. 15:780-789.

Schirawski, J., Mannhaupt, G., Münch, K., Brefort, T., Schipper, K., Doehlemann, G., Di Stasio, M., Rössel, N., Mendoza-Mendoza, A., Pester, D., Müller, O., Winterberg, B., Meyer, E., Ghareeb, H., Wollenberg, T., Münsterkötter, M., Wong, P., Walter, M., Stukenbrock, E., Güldener, U., and Kahmann, R. 2010. Pathogenicity determinants in smut fungi revealed by genome comparison. Science 330:1546-1548.

Schulz, B., Banuett, F., Dahl, M., Schlesinger, R., Schäfer, W., Martin, T., Herskowitz, I., and Kahmann, R. 1990. The *b* alleles of *U. maydis*, whose combinations program pathogenic development, code for polypeptides containing a homeodomain-related motif. Cell 60:295-306.

Schurack, S., Depotter, J. R. L., Gupta, D., Thines, M., and Doehlemann, G. 2021. Comparative transcriptome profiling identifies maize line specificity of fungal effectors in the maize-*Ustilago maydis* interaction. Plant J. 106:733-752.

Schuster, M., Schweizer, G., and Kahmann, R. 2018. Comparative analyses of secreted proteins in plant pathogenic smut fungi and related basidiomycetes. Fungal Genet. Biol. 112:21-30.

Schuster, M., Schweizer, G., Reissmann, S., and Kahmann, R. 2016. Genome editing in *Ustilago maydis* using the CRISPR-Cas system. Fungal Genet. Biol. 89:3-9.

Schweizer, G., Münch, K., Mannhaupt, G., Schirawski, J., Kahmann, R., and Dutheil, J. Y. 2018. Positively selected effector genes and their contribution to virulence in the smut fungus *Sporisorium reilianum*. Genome Biol. Evol. 10:629-645.

Seitner, D., Uhse, S., Gallei, M., and Djamei, A. 2018. The core effector Cce1 is required for early infection of maize by *Ustilago maydis*. Mol. Plant Pathol. 19:2277-2287.

Seong, K., and Krasileva, K. V. 2023. Prediction of effector protein structures from fungal phytopathogens enables evolutionary analyses. Nat. Microbiol. 8:174-187.

Sharma, R., Mishra, B., Runge, F., and Thines, M. 2014. Gene loss rather than gene gain is associated with a host jump from monocots to dicots in the smut fungus *Melanopsichium pennsylvanicum*. Genome Biol. Evol. 6:2034-2049.

Sharma, R., Ökmen, B., Doehlemann, G., and Thines, M. 2019. Saprotrophic yeasts formerly classified as *Pseudozyma* have retained a large effector arsenal, including functional Pep1 orthologs. Mycol. Prog. 18:763-768.

Sharma, R., Xia, X., Riess, K., Bauer, R., and Thines, M. 2015. Comparative genomics including the early-diverging smut fungus *Ceraceosorus bombacis* reveals signatures of parallel evolution within plant and animal pathogens of fungi and oomycetes. Genome Biol. Evol. 7:2781-2798.

Slater, G. S. C., and Birney, E. 2005. Automated generation of heuristics for biological sequence comparison. BMC Bioinf. 6:31.

Stanke, M., Keller, O., Gunduz, I., Hayes, A., Waack, S., and Morgenstern, B. 2006. AUGUSTUS: Ab initio prediction of alternative transcripts. Nucleic Acids Res. 34:W435-W439.

Stirnberg, A., and Djamei, A. 2016. Characterization of ApB73, a virulence factor important for colonization of *Zea mays* by the smut *Ustilago maydis*. Mol. Plant Pathol. 17:1467-1479.

Tanaka, S., Brefort, T., Neidig, N., Djamei, A., Kahnt, J., Vermerris, W., Koenig, S., Feussner, K., Feussner, I., and Kahmann, R. 2014. A secreted *Ustilago maydis* effector promotes virulence by targeting anthocyanin biosynthesis in maize. eLife 3:e01355.

Tanaka, S., Gollin, I., Rössel, N., and Kahmann, R. 2020. The functionally conserved effector Sta1 is a fungal cell wall protein required for virulence in *Ustilago maydis*. New Phytol. 227:185-199.

Tanaka, S., Schweizer, G., Rössel, N., Fukada, F., Thines, M., and Kahmann, R. 2019. Neofunctionalization of the secreted Tin2 effector in the fungal pathogen *Ustilago maydis*. Nat. Microbiol. 4:251-257.

Ter-Hovhannisyan, V., Lomsadze, A., Chernoff, Y. O., and Borodovsky, M. 2008. Gene prediction in novel fungal genomes using an ab initio algorithm with unsupervised training. Genome Res. 18:1979-1990.

Tollot, M., Assmann, D., Becker, C., Altmüller, J., Dutheil, J. Y., Wegner, C.-E., and Kahmann, R. 2016. The WOPR protein Ros1 is a master regulator of sporogenesis and late effector gene expression in the maize pathogen *Ustilago maydis*. PLoS Pathog. 12:e1005697.

Uhse, S., and Djamei, A. 2018. Effectors of plant-colonizing fungi and beyond. PLoS Pathog. 14:e1006992.

Uhse, S., Pflug, F. G., Stirnberg, A., Ehrlinger, K., von Haeseler, A., and Djamei, A. 2018. In vivo insertion pool sequencing identifies virulence factors in a complex fungal-host interaction. PLoS Biol. 16:e2005129.

van Kempen, M., Kim, S. S., Tumescheit, C., Mirdita, M., Lee, J., Gilchrist, C. L. M., Söding, J., and Steinegger, M. 2024. Fast and accurate protein structure search with Foldseek. Nat. Biotechnol. 42:243-246.

Vánky, K. 2013. Illustrated Genera of Smut Fungi. American Phytopathological Society, St. Paul, MN.

Varadi, M., Anyango, S., Deshpande, M., Nair, S., Natassia, C., Yordanova, G., Yuan, D., Stroe, O., Wood, G., Laydon, A., Žídek, A., Green, T.,

Tunyasuvunakool, K., Petersen, S., Jumper, J., Clancy, E., Green, R., Vora, A., Lutfi, M., Figurnov, M., Cowie, A., Hobbs, N., Kohli, P., Kleywegt, G., Birney, E., Hassabis, D., and Velankar, S. 2022. AlphaFold Protein Structure Database: Massively expanding the structural coverage of protein-sequence space with high-accuracy models. Nucleic Acids Res. 50:D439-D444.

Walter, M. C., Rattei, T., Arnold, R., Güldener, U., Münsterkötter, M., Nenova, K., Kastenmüller, G., Tischler, P., Wölling, A., Volz, A., Pongratz, N., Jost, R., Mewes, H.-W., and Frishman, D. 2009. PEDANT covers all complete RefSeq genomes. Nucleic Acids Res. 37:D408-D411.

Wang, S., Boevink, P. C., Welsh, L., Zhang, R., Whisson, S. C., and Birch, P. R. J. 2017. Delivery of cytoplasmic and apoplastic effectors from *Phytophthora infestans* haustoria by distinct secretion pathways. New Phytol. 216:205-215.

Weiland, P., Dempwolff, F., Steinchen, W., Freibert, S.-A., Tian, H., Glatter, T., Martin, R., Thomma, B. P. H. J., Bange, G., and Altegoer, F. 2023. Structural and functional analysis of the cerato-platanin-like protein Cpl1 suggests diverging functions in smut fungi. Mol. Plant Pathol. 24:768-787.

Win, J., Chaparro-Garcia, A., Belhaj, K., Saunders, D. G. O., Yoshida, K., Dong, S., Schornack, S., Zipfel, C., Robatzek, S., Hogenhout, S. A., and Kamoun, S. 2012. Effector biology of plant-associated organisms: Concepts and perspectives. Cold Spring Harb. Symp. Quant. Biol. 77: 235-247.

Xia, W., Yu, X., and Ye, Z. 2020. Smut fungal strategies for the successful infection. Microb. Pathog. 142:104039.

Yan, X., Tang, B., Ryder, L. S., MacLean, D., Were, V. M., Eseola, A. B., Cruz-Mireles, N., Ma, W., Foster, A. J., Osés-Ruiz, M., and Talbot, N. J. 2023. The transcriptional landscape of plant infection by the rice blast fungus *Magnaporthe oryzae* reveals distinct families of temporally co-regulated and structurally conserved effectors. Plant Cell 35:1360-1385.

Ye, Z., Pan, Y., Zhang, Y., Cui, H., Jin, G., McHardy, A. C., Fan, L., and Yu, X. 2017. Comparative whole-genome analysis reveals artificial selection effects on *Ustilago esculenta* genome. DNA Res. 24:635-648.

Yu, D. S., Outram, M. A., Smith, A., McCombe, C. L., Khambalkar, P. B., Rima, S. A., Sun, X., Ma, L., Ericsson, D. J., Jones D. A., and Williams, S. J. 2024. The structural repertoire of *Fusarium oxysporum* f. sp. *lycopersici* effectors revealed by experimental and computational studies. eLife 12:RP89280.

Zambanini, T., Buescher, J. M., Meurer, G., Wierckx, N., and Blank, L. M. 2016. Draft genome sequence of *Ustilago trichophora* RK089, a promising malic acid producer. Genome Announc. 4:e00749-16.

Zuo, W., Depotter, J. R. L., Gupta, D. K., Thines, M., and Doehlemann, G. 2021. Cross-species analysis between the maize smut fungi *Ustilago maydis* and *Sporisorium reilianum* highlights the role of transcriptional change of effector orthologs for virulence and disease. New Phytol. 232:719-733.

Zuo, W., Depotter, J. R. L., Stolze, S. C., Nakagami, H., and Doehlemann, G. 2023. A transcriptional activator effector of *Ustilago maydis* regulates hyperplasia in maize during pathogen-induced tumor formation. Nat Commun. 14:6722.

Zuo, W., Ökmen, B., Depotter, J. R. L., Ebert, M. K., Redkar, A., Misas Villamil, J., and Doehlemann, G. 2019. Molecular interactions between smut fungi and their host plants. Annu. Rev. Phytopathol. 57: 411-430.